# Wavelet-ANN Based Detection of Fault Location of Hybrid Renewable Energy Sources Connected Power Transmission System

S. Chandra Shekar*‡, T. Muthamizhan**, Mohammad Aijaz***, D.Chandra Sekhar****

*Professor, Department of EEE, NRI Institute of Technology, Vijayawada, India.

**Associate Professor, Department of EEE, Sri Sai Ram Institute of Technology, Chennai, India.

***Associate Professor, Department of EEE, Kodada Institute of Technology and Science for Women, Kodad, Telangana, India.

****Assistant Professor, Department of EEE, Malla Reddy Engineering College, Maisammaguda, Secunderabad, Telangana, India.

(chandrasekharsavarapu@gmail.com, muthamizhan@gmail.com, aijaz.vsce@gmail.com, daram.sekhar@gmail.com)

‡Corresponding Author; S. Chandra Shekar*, , Anurag Engineering College, Kodad, Telangana, India.

Tel: +91 9553122273, chandrasekharsavarapu@gmail.com.

*Received: 30.06.2023 Accepted:05.08.2023*

**Abstract:** The complexity of the power system increases as the hundreds of lines involved due to the penetration of conventional and renewable energy sources to meet the increased load demand. Transmitting the power for hundreds of kilometres long distances makes complexity in the network to locate the fault. Thus it is necessary to develop suitable algorithms to identify the location of the fault accurately in presence of large number of transmission lines. In this paper a novel Wavelet Artificial Neural Network (WANN) based method is developed where the Detailed coefficients (D1 coefficients) obtained from the current signals are used for training and testing ANN. The fault location is carried out in presence of renewable energy sources for various distances, fault impedances on 4-bus connected transmission system. A 4-bus transmission system is simulated using simulation software and the analysis of fault is done by using current signals of various faults with the help of wavelet multi-resolution analysis at both buses. This analysis is worked out almost within half cycle. The proposed wavelet based algorithm is tested for all fault conditions in presence of renewable energy sources with different power ratings at various distances and hence it is proved that the proposed method provided the best results for different fault impedances, fault generator capacities, fault inception angles (FIA).

***Keywords:*** D1 coefficients, Wavelet-ANN, Bior1.5 mother wavelet, fault inception angle, fault impedance.

## 1.

## 2. Introduction

The power system is designed to supply continuous power to the end customers without changing voltage, current and frequency levels with minimal cost. But, due to huge penetration of loads to the existing power system, we need to identify the location of disturbances occurring during faults conditions as early as possible and to be cleared using circuit breakers [1].

Here some recent papers are discussed with various techniques for the fault location.

Mahmood Parsia, et al proposes four fault location techniques namely, time-domain, impedance, visual inspection and a novel wavelet-based technique [2]. Dr. H. V. Gururaja Rao et al a new, simple and dependable wavelet transform based fault location estimator for transmission lines deploying STATCOM integrating energy storage device [3]. Majid Jamila, Abul Kalama, A.Q. Ansaria, M. Rizwanba presented a novel method of wavelet transform along with a generalized neural network for fault location estimation 2-bus system transmission lines. The fault location accuracy is changing with respect to type fault and the error is more than 2.5% [4]. A. Salehi Dobakhshari and A. M. Ranjbar studied the a Linear Weighted Least-Squares (LWLS) method for fault location on transmission lines by synchronized measurements voltage western systems coordinating council on 9-bus, 22-bus transmission system. The accuracy corresponds to line 18–21 are least with 3% error [5]. Nabamita Roy and Kesab Bhattacharya proposed a method of fault location identification using frequency components of S-Matrices. These components are used as input for the ANN for training the network. A back propagation ANN is used to find fault location. It found the fault location with an error of 4.46% [6]. Alkım Capar, Aysen Basa Arsoy proposed a fault location method using fault voltage and currents vectors on both ends of transmission line measurements and line parameters. It is found that if the fault is closed at the location of the capacitor the error becomes increasing [7]. Kunjin Chen, Caowei Huang, Jinliang He discussed fault detection techniques using feature extraction from the signal to be analyzed. A D1 review of the methods is discussed for the fault detection, classification and location in transmission and distribution systems. The fault location maximum error was 5% [8]. J. Ren, Member, S. S. Venkata, and E. Sortomme proposed Synchrophasor measurements in distribution systems for the location of the fault in 14-bus distribution feeder. The 1% of change in current and voltage phasor will change the estimated distance value error by 2% [9]. Gaurav Kapoor proposed a scheme for determining the fault location on a 2-bus transmission system using discrete wavelet transform using current signals on both ends of the lines. The fault location error is a maximum of 2.5% [10]. From the above literature survey, few limitations have been observed in fault location. The identification of fault location is dependent on the distance at which the fault occurs in the transmission line. Also, the estimated error of fault location is very high.

In this paper a novel WANN based method is developed where the wavelet multi resolution analysis is used to obtain D1 from the fault current signals and this data is used for training and testing ANN. The fault location is carried out in presence of conventional and renewable energy sources on 4-bus connected transmission system. A 4-bus transmission system is simulated using simulation software and the analysis of fault is done by using current signals of various faults. This analysis is worked out almost within half cycle of current signals. The proposed WANN based algorithm is tested for all fault conditions with different power ratings of conventional and renewable energy sources at various distances. Hence it is proved that the proposed method provided the best results for the fault location at different fault impedances, generator capacities, and fault inception angles.

## 3. Wavelets

A wavelet is a small wave, which has finite energy concentrated over a time interval has scaling and shifty properties to suit any type of transient time-frequency varying signals which provides time-frequency localization of a signal having abrupt changes. The mother wavelet is able to the translated and dilated discretely. However, the Wavelet Transform (WT) uses variable window widths (short for high frequencies and longs for low frequencies) and allows in general obtaining adequate information combining the temporal event with the frequency spectrum [11]. Therefore, it has been selected as an analysis tool. Wavelets are used in the series expansion of functions or signals much similar to the Fourier series [12]. A wave and wavelet is shown in Fig.1.

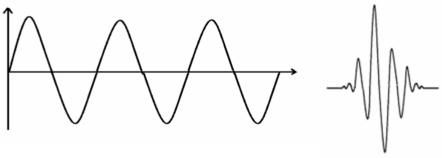

**Fig.1.** A wave and wavelet

The various types of wavelets are shown in Fig.2. Among these wavelets, the Bior1.5 wavelet is considered because of its unique feature of producing symmetrical coefficients as output from the transient signals [13].

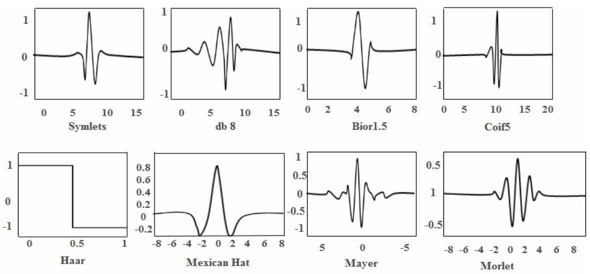


**Fig.2.** Types of wavelets

## 4. Artificial Neural Network Structure

ANN's are playing a very crucial role in electrical Power systems applications. Multilayer networks are one among them used for applications of Electrical Power systems. A multilayer neural network consists of more than one layer. Introduction of hidden layers improves the problem solving capability of the network. The general architecture of the Neural Network employed for the proposed fault location algorithm [14] is shown in fig.3.

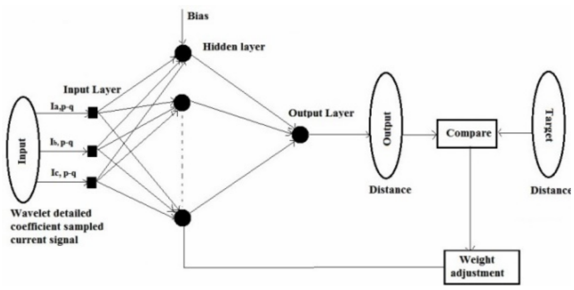


**Fig.3.** Neural Network Structure.

This network is trained using error back propagation training algorithm. In this training algorithm inputs are presented to the network and outputs of all layers are calculated in the forward direction and error is calculated by comparing the output with the target output and then weights are updated in the backward direction that is weights of output layer are updated first then hidden layer weights based on the error value till the weights of neurons are stabilized. The number of training parameters and training sets is depending on the type of application. The parameter selection plays a vital role in the stabilization of weights. The main parameters to be selected are

- Initial weights
- Learning coefficient

Weights initiation should be done properly to get the final weights to be stabilized with minimum error. If the initial weights are not selected properly the error may be trapped into local minima or sometimes the weights may not be converged so the training is to be restarted. Similarly, the learning coefficient (usually small) is also to be selected at a small value so that weights will be converged with minimum error. The ANN parameters used for this work are

Input data: D1 coefficients of post fault current signals

Target data: Line distance

Number of layers:2

Training algorithm: Back-propagation

Number of Patterns:

*(Distances-5, Number of faults-4, Number of buss-4, FIA's-9)*

Forward pass

Output=

where,

D1 coefficients of phase-A on $p^{th}$ bus at $q^{th}$ FIA

D1 coefficients of phase-B on $p^{th}$ bus at $q^{th}$ FIA

D1 coefficients of phase-C on $p^{th}$ bus at $q^{th}$ FIA

Where,

P = buss (B1, T2, T3, T4)

q = FIAs ($0^0$, $20^0$, $40^0$, $60^0$, $80^0$, $100^0$, $120^0$, $140^0$, $160^0$)

Activation sigmoid function

AFL is Authentic Fault Location

EFL is Evaluated Fault Location

TLL is Total Line Length.

## 5. Wavelet-Based Algorithm for the Preparation of Training and Testing Patterns

The proposed wavelet based algorithm is designed for obtaining training and testing patterns of D1 coefficients from the current signals at different distances 10km, 20km, 30km, 40km, 50km for Bus1, Bus2 and 1km, 2km, 3km, 4km, 5km for Bus3, Bus4 at FIAs $0^0$, $20^0$, $40^0$, $60^0$, $80^0$, $100^0$, $120^0$, $140^0$, $160^0$. After D1 coefficients are obtained, these values given as inputs for ANN and location of fault as target output. Further, the actual distance of fault location is compared with ANN distance. In this paper Bior1.5 wavelet horizontal D1 coefficients of absolute values are used for the analysis.

***<u>Designing algorithm</u>***

Step-1: Set the bus numbers where the fault is to be analyzed.
Step-2: Apply the fault and measure all the currents of all phases at both ends.
Step-3: Decompose the current signals of each phase by applying the Bior1.5 mother wavelet for all the lines.
Step-4: Obtain the D1 coefficients of current signals.
Step-5: Obtain the absolute value of D1 coefficients.
Step-6: Set the threshold value.
Step-7: Training ANN with D1 coefficients.

Fig.4. shown flowchart of the proposed algorithm.

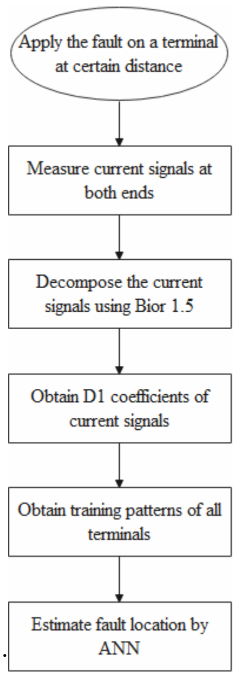


*Fig.4. Flowchart of Proposed algorithm.*

## 6. Wavelet-ANN Based Technique for Fault Location

A 4-bus renewable energy sources connected transmission system is simulated with 3 different generating capacities show in Table.1.

**Table.1.** System Data

| | | |
|---|---|---|
| Bus1 | Conventional source | 100MVA |
| Bus2 | Utility grid | 2500MVA |
| Bus3 | Wind energy source | No.of wind turbines:6, Power rating: 10MW |
| Bus4 | Solar PV source | PV cell Power Rating: 1MW |

The proposed 4-bus renewable energy sources connected transmission system is considered for the analysis and shown in fig.5.

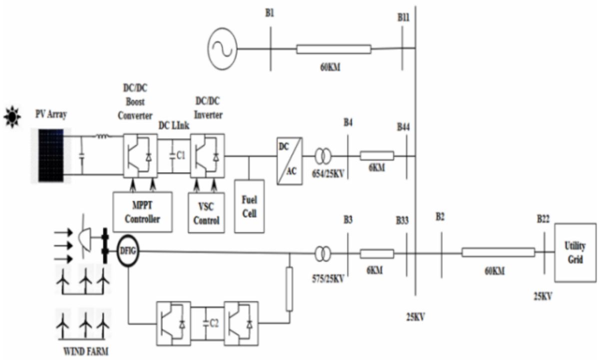


**Fig.5.** Single line diagram of 4-bus connected transmission system

Line length for Bus1 and Bus2 is 60km line where as for Bus3 and Bus4 is 6km. Symmetrical and unsymmetrical faults are applied to the lines at different distances.

System frequency = 60Hz

Time per cycle ==16.6 (msec)

Sample time = =(sec)

Total 216000 samples are considered per cycle. Bior1.5 mother wavelet-based algorithm extracts D1 coefficients from current signals. The different types of faults are created at various distances with several fault inception angles in this section. The fault currents are obtained for all these cases and wavelet analysis has been carried out. The D1 coefficients obtained from the wavelet-based algorithm are used for training ANN. After the ANN is trained, it has been tested for different scenarios using the testing data. The testing data contains different faults occurring at several fault inception angles at various distances. The results are presented in section-6.

## 6. Fault Analysis of 4-bus Renewable Energy Sources Connected Transmission System

The fault analysis with LG, LLG, LL and 3-phase faults on Bus1, Bus2, Bus3 and Bus4 are discussed below.

### Training data at B1 with LG (AG) fault

To prepare the necessary training and testing data an LG fault is applied on phase-A at B1 at different distances of 10km, 20km, 30km, 40km, 50km with several FIAs such as $0^o$, $20^o$, $40^o$, $60^o$, $80^o$, $100^o$, $120^o$, $140^o$, $160^o$and measured the all the phases current signals. The D1 coefficients of all phase currents have been computed as given in Table.1-3. From Table.1-3 it can be observed that the D1 coefficient values corresponding to phase-A have relatively higher compared with phase-B and phase-C. All these D1 coefficient values obtained at various distances and FIA's with different faults are used to train ANN with target value as distance. An example of the training pattern is given below.

### Training patterns at B1 with LG (AG) fault

Training patterns are formed with the help of data from Table.2-4.

Example: Consider a distance of 10km and FIA as $0^o$. From Table.2-4 take the D1 coefficients corresponding to phase-A, phase-B and phase-C currents. Thus the first training pattern is formed with $I_{a,B1-0}$ = 1052.7, $I_{b,B1-0}$ = 6.03, $I_{c,B1-0}$ = 1.681 as inputs and the distance 10km as target. Similarly, train ANN and corresponding training patterns are given in Table.5. The location error of actual distance and ANN distance using training data and training patterns is given in Table.6. The location absolute error between the AFL and EFL for LG, LLG, 3-phase and LL faults are 1.66 (max.), -1.64 (max.), 1.66 (max.) and 1.33(max.).

Table.2. D1 coefficients of phase-A current at various distances and FIA at B1

| FIA/Km | $0^0$ | $20^0$ | $40^0$ | $60^0$ | $80^0$ | $100^0$ | $120^0$ | $140^0$ | $160^0$ |
|---|---|---|---|---|---|---|---|---|---|
| **10** | 1052.7 | 1061.9 | 939.32 | 999.59 | 1032.8 | 929.19 | 892.69 | 946.96 | 1065.3 |
| **20** | 773.49 | 793.01 | 700.37 | 764.4 | 820.98 | 731.32 | 697.35 | 735.75 | 820.0 |
| **30** | 694.71 | 692.04 | 682.22 | 685.35 | 732.52 | 654.65 | 620.94 | 648.86 | 723.7 |
| **40** | 653.38 | 651.87 | 667.89 | 667.68 | 725.18 | 656.29 | 622.11 | 641.98 | 712.2 |
| **50** | 628.98 | 640.54 | 638.08 | 720.49 | 771.52 | 690.42 | 656.80 | 687.57 | 769.8 |

**Table.3.** D1 coefficients of phase-B current at various distances and FIA at B1

| FIA/Km | $0^0$ | $20^0$ | $40^0$ | $60^0$ | $80^0$ | $100^0$ | $120^0$ | $140^0$ | $160^0$ |
|---|---|---|---|---|---|---|---|---|---|
| **10** | 6.03 | 8.362 | 2.028 | 9.904 | 9.468 | 6.453 | 7.195 | 5.838 | 5.802 |
| **20** | 5.05 | 7.615 | 6.021 | 6.989 | 5.654 | 4.490 | 5.368 | 5.394 | 3.726 |
| **30** | 4.12 | 9.559 | 3.929 | 3.454 | 3.448 | 3.581 | 3.613 | 2.879 | 2.716 |
| **40** | 2.91 | 7.016 | 6.201 | 5.355 | 3.804 | 5.265 | 5.885 | 5.654 | 7.251 |
| **50** | 9.97 | 1.617 | 6.013 | 4.297 | 3.602 | 3.780 | 4.015 | 2.935 | 3.094 |

**Table.4.** D1 coefficients of phase-C current at various distances and FIA at B1

| FIA/Km | $0^0$ | $20^0$ | $40^0$ | $60^0$ | $80^0$ | $100^0$ | $120^0$ | $140^0$ | $160^0$ |
|---|---|---|---|---|---|---|---|---|---|
| **10** | 1.681 | 2.508 | 3.869 | 8.834 | 8.934 | 7.790 | 6.551 | 5.845 | 4.639 |
| **20** | 2.458 | 5.993 | 3.071 | 7.671 | 5.811 | 6.528 | 6.296 | 6.440 | 5.118 |
| **30** | 7.340 | 6.536 | 4.990 | 3.445 | 3.254 | 3.006 | 3.062 | 3.326 | 3.353 |
| **40** | 1.352 | 2.514 | 3.504 | 6.275 | 3.414 | 1.844 | 2.038 | 2.710 | 3.732 |
| **50** | 6.374 | 1.438 | 2.325 | 4.782 | 4.123 | 3.934 | 3.336 | 3.020 | 3.718 |

**Table.5.** Training patterns

| Bus(p)-FIA(q) | Ia,p-q | Ib,p-q | Ic,p-q | Target distance |
|---|---|---|---|---|
| B1-$0^0$ | 1052.7 | 6.03 | 1.681 | 10 |
| B1-$20^0$ | 1061.9 | 8.362 | 2.508 | |
| B1-$40^0$ | 939.32 | 2.028 | 3.869 | |
| B1-$60^0$ | 999.59 | 9.904 | 8.834 | |
| B1-$80^0$ | 1032.8 | 9.468 | 8.934 | |
| B1-$100^0$ | 929.19 | 6.453 | 7.79 | |
| B1-$120^0$ | 892.69 | 7.195 | 6.551 | |
| B1-$140^0$ | 946.96 | 5.838 | 5.845 | |
| B1-$160^0$ | 1065.73 | 5.802 | 4.639 | |
| B1-$0^0$ | 773.49 | 773.49 | 2.458 | 20 |
| B1-$20^0$ | 793.01 | 793.01 | 5.993 | |
| B1-$40^0$ | 700.37 | 700.37 | 3.071 | |
| B1-$60^0$ | 764.4 | 764.4 | 7.671 | |
| B1-$80^0$ | 820.98 | 820.98 | 5.811 | |
| B1-$100^0$ | 731.32 | 731.32 | 6.528 | |
| B1-$120^0$ | 697.35 | 697.35 | 6.296 | |

| | | | | |
|---|---|---|---|---|
| B1-140$^{0}$ | 735.75 | 735.75 | 6.44 | |
| B1-160$^{0}$ | 820.01 | 820.01 | 5.118 | |
| B1-0$^{0}$ | 694.71 | 4.12 | 7.34 | 30 |
| B1-20$^{0}$ | 692.04 | 9.559 | 6.536 | |
| B1-40$^{0}$ | 682.22 | 3.929 | 4.99 | |
| B1-60$^{0}$ | 685.35 | 3.454 | 3.445 | |
| B1-80$^{0}$ | 732.52 | 3.448 | 3.254 | |
| B1-100$^{0}$ | 654.65 | 3.581 | 3.006 | |
| B1-120$^{0}$ | 620.94 | 3.613 | 3.062 | |
| B1-140$^{0}$ | 648.86 | 2.879 | 3.326 | |
| B1-160$^{0}$ | 723.75 | 2.716 | 3.353 | |
| B1-0$^{0}$ | 653.38 | 2.91 | 1.352 | 40 |
| B1-20$^{0}$ | 651.87 | 7.016 | 2.514 | |
| B1-40$^{0}$ | 667.89 | 6.201 | 3.504 | |
| B1-60$^{0}$ | 667.68 | 5.355 | 6.275 | |
| B1-80$^{0}$ | 725.18 | 3.804 | 3.414 | |
| B1-100$^{0}$ | 656.29 | 5.265 | 1.844 | |
| B1-120$^{0}$ | 622.11 | 5.885 | 2.038 | |
| B1-140$^{0}$ | 641.98 | 5.654 | 2.71 | |
| B1-160$^{0}$ | 712.23 | 7.251 | 3.732 | |
| B1-0$^{0}$ | 628.98 | 9.97 | 6.374 | 50 |
| B1-20$^{0}$ | 640.54 | 1.617 | 1.438 | |
| B1-40$^{0}$ | 638.08 | 6.013 | 2.325 | |
| B1-60$^{0}$ | 720.49 | 4.297 | 4.782 | |
| B1-80$^{0}$ | 771.52 | 3.602 | 4.123 | |
| B1-100$^{0}$ | 690.42 | 3.78 | 3.934 | |
| B1-120$^{0}$ | 656.8 | 4.015 | 3.336 | |
| B1-140$^{0}$ | 687.57 | 2.935 | 3.02 | |
| B1-160$^{0}$ | 769.87 | 3.094 | 3.718 | |

**Table.6.** Wavelet-ANN based fault location

| Type Fault | Actual Distance (km) | ANN Distance (km) | | | % error | | |
|---|---|---|---|---|---|---|---|
| | | B1 | | | | | |
| LG (AG) | 10 | 9.68 | | | 0.53 | | |
| | 20 | 21 | | | -1.66 | | |
| | 30 | 30.96 | | | -1.6 | | |
| | 40 | 39.2 | | | 1.33 | | |
| | 50 | 49.7 | | | 0.5 | | |
| LLG (ACG) | 10 | 9.72 | 11 | | 0.46 | -1.64 | |
| | 20 | 19.8 | 19.58 | | 0.2 | 0.7 | |
| | 30 | 29.6 | 30.65 | | 0.66 | -1.08 | |
| | 40 | 39 | 40.80 | | 1.66 | -1.33 | |
| | 50 | 49 | 49.76 | | 1.66 | 0.4 | |
| 3-phase | 10 | 10.7 | 11 | 10.8 | -1.3 | -1.6 | -1.33 |
| | 20 | 19.6 | 19.4 | 19.2 | 0.6 | 1 | 1.33 |
| | 30 | 29.6 | 31.1 | 30.2 | 0.6 | -1.8 | -0.33 |
| | 40 | 40.5 | 41.8 | 38.2 | -0.9 | -0.3 | 0.93 |
| | 50 | 49 | 49.8 | 49.1 | 1.6 | 0.33 | 1.5 |
| LL (AB) | 10 | 9.68 | 10.8 | | 0.53 | -1.33 | |
| | 20 | 19.72 | 19.4 | | 0.46 | 1 | |
| | 30 | 29.2 | 30.8 | | 1.33 | -1.33 | |
| | 40 | 39.3 | 39.5 | | 1.16 | 0.833 | |
| | 50 | 9.68 | 10.8 | | 0.53 | -1.33 | |

**Training data at B1 with LLG (ACG) fault**

Apply LLG fault on phase-A and phase-C at B1 with different distances 10km, 20km, 30km, 40km, 50km and FIAs $0^0$, $20^0$, $40^0$, $60^0$, $80^0$, $100^0$, $120^0$, $140^0$, $160^0$and measure current signals as D1 coefficients at all phases as given in Table.7-9.

**Table.7.** D1 coefficients of phase-A current at various distances and FIA at B1

| FIA/ Km | $0^0$ | $20^0$ | $40^0$ | $60^0$ | $80^0$ | $100^0$ | $120^0$ | $140^0$ | $160^0$ |
|---|---|---|---|---|---|---|---|---|---|
| 10 | 928.3 | 984.90 | 945.00 | 992.21 | 1039.4 | 1163.16 | 1077.62 | 987.96 | 990.44 |
| 20 | 839.7 | 889.16 | 782.12 | 735.74 | 765.7 | 854.32 | 808.05 | 736.54 | 731.59 |
| 30 | 678.7 | 711.05 | 710.26 | 586.96 | 612.0 | 686.45 | 651.93 | 592.55 | 587.96 |
| 40 | 655.2 | 692.38 | 651.09 | 476.87 | 512.5 | 565.15 | 538.79 | 479.88 | 481.89 |
| 50 | 654.0 | 611.57 | 624.42 | 427.97 | 450.0 | 505.49 | 471.74 | 431.03 | 429.31 |

**Table.8.** D1 coefficients of phase-B current at various distances and FIA at B1

| FIA/Km | $0^0$ | $20^0$ | $40^0$ | $60^0$ | $80^0$ | $100^0$ | $120^0$ | $140^0$ | $160^0$ |
|---|---|---|---|---|---|---|---|---|---|
| 10 | 4.284 | 3.8295 | 4.2658 | 6.5004 | 6.3729 | 5.0435 | 6.12 | 5.77 | 6.013 |
| 20 | 2.574 | 2.521 | 3.2096 | 9.4736 | 8.1494 | 8.3832 | 7.16 | 6.32 | 8.205 |
| 30 | 3.588 | 2.5518 | 3.9864 | 11.6215 | 8.5848 | 8.0602 | 4.74 | 4.24 | 6.745 |
| 40 | 8.503 | 2.5822 | 9.2304 | 5.4278 | 5.2256 | 3.7492 | 5.07 | 5.36 | 5.647 |
| 50 | 8.534 | 4.5822 | 2.2304 | 8.6158 | 7.9212 | 8.1636 | 7.14 | 6.39 | 7.853 |

**Table.9.** D1 coefficients of phase-C current at various distances and FIA at B1

| FIA/Km | $0^0$ | $20^0$ | $40^0$ | $60^0$ | $80^0$ | $100^0$ | $120^0$ | $140^0$ | $160^0$ |
|---|---|---|---|---|---|---|---|---|---|
| 10 | 955.18 | 962.59 | 973.23 | 1003.76 | 1110.11 | 988.25 | 932.27 | 961.31 | 1064.07 |
| 20 | 737.27 | 816.71 | 908.54 | 775.06 | 861.96 | 801.14 | 739.65 | 745.83 | 810.09 |
| 30 | 645.08 | 680.98 | 755.25 | 663.87 | 729.02 | 710.79 | 648.93 | 638.47 | 680.79 |
| 40 | 634.6 | 671.56 | 677.63 | 622.13 | 682.49 | 686.60 | 630.76 | 619.39 | 656.15 |
| 50 | 604.8 | 603.36 | 659.42 | 661.33 | 720.56 | 725.43 | 663.35 | 647.26 | 677.39 |

Table.7-9 it is observed that the D1 coefficient values correspond to phase-A has relatively higher values compared with phase-B and phase-C. All these D1 coefficient values obtained at various distances, various FIA's with different faults are used to train ANN with target value as distance.

**Training patterns at B1 with LLG (ACG) fault**

Example: Consider a distance of 10km and FIA as $0^0$. From the Table.7-9 take the D1 coefficients corresponding to phase-A, phase-B and phase-C. Thus the first training pattern is formed with $I_{a,p-q}$ = 928.3, $I_{b,p-q}$ = 4.2848, $I_{c,p-q}$ = 955.18 as inputs and the distance 10km as target. Similarly, train ANN with all data given in Table.10 gives the fault location.

**Table.10.** Training patterns for 10km distance

| Terminal(p)-FIA(q) | Ia,p-q | Ib,p-q | Ic,p-q | Target distance |
|---|---|---|---|---|
| B1-$0^0$ | 928.3 | 4.2848 | 955.18 | 10 |
| B1-$20^0$ | 984.9 | 3.8295 | 962.59 | |
| B1-$40^0$ | 945 | 4.2658 | 973.23 | |
| B1-$60^0$ | 992.21 | 6.5004 | 1003.76 | |
| B1-$80^0$ | 1039.45 | 6.3729 | 1110.11 | |
| B1-$100^0$ | 1163.16 | 5.0435 | 988.25 | |
| B1-$120^0$ | 1077.62 | 6.1257 | 932.27 | |
| B1-$140^0$ | 987.96 | 5.7767 | 961.31 | |
| B1-$160^0$ | 990.44 | 6.0138 | 1064.07 | |
| B1-$0^0$ | 839.7 | 2.5747 | 737.27 | 20 |
| B1-$20^0$ | 889.16 | 2.521 | 816.71 | |
| B1-$40^0$ | 782.12 | 3.2096 | 908.54 | |
| B1-$60^0$ | 735.74 | 9.4736 | 775.06 | |
| B1-$80^0$ | 765.75 | 8.1494 | 861.96 | |
| B1-$100^0$ | 854.32 | 8.3832 | 801.14 | |
| B1-$120^0$ | 808.05 | 7.1476 | 739.65 | |
| B1-$140^0$ | 736.54 | 6.3622 | 745.83 | |
| B1-$160^0$ | 731.59 | 8.2054 | 810.09 | |
| B1-$0^0$ | 678.7 | 3.5887 | 645.08 | 30 |
| B1-$20^0$ | 711.05 | 2.5518 | 680.98 | |
| B1-$40^0$ | 710.26 | 3.9864 | 755.25 | |
| B1-$60^0$ | 586.96 | 11.6215 | 663.87 | |
| B1-$80^0$ | 612.7 | 8.5848 | 729.02 | |
| B1-$100^0$ | 686.45 | 8.0602 | 710.79 | |
| B1-$120^0$ | 651.93 | 4.7574 | 648.93 | |
| B1-$140^0$ | 592.55 | 4.8924 | 638.47 | |
| B1-$160^0$ | 587.96 | 6.7455 | 680.79 | |
| B1-$0^0$ | 655.2 | 8.5034 | 634.6 | 40 |
| B1-$20^0$ | 692.38 | 2.5822 | 671.56 | |
| B1-$40^0$ | 651.09 | 9.2304 | 677.63 | |
| B1-$60^0$ | 476.87 | 5.4278 | 622.13 | |
| B1-$80^0$ | 512.35 | 5.2256 | 682.49 | |
| B1-$100^0$ | 565.15 | 3.7492 | 686.6 | |
| B1-$120^0$ | 538.79 | 5.5207 | 630.76 | |
| B1-$140^0$ | 479.88 | 5.6636 | 619.39 | |
| B1-$160^0$ | 481.89 | 5.6477 | 656.15 | |
| B1-$0^0$ | 654 | 8.5034 | 604.8 | 50 |
| B1-$20^0$ | 611.57 | 4.5822 | 603.36 | |
| B1-$40^0$ | 624.42 | 2.2304 | 659.42 | |
| B1-$60^0$ | 427.97 | 8.6158 | 661.33 | |
| B1-$80^0$ | 450 | 7.9212 | 720.56 | |
| B1-$100^0$ | 505.49 | 8.1636 | 725.43 | |
| B1-$120^0$ | 471.74 | 7.6314 | 663.35 | |
| B1-$140^0$ | 431.03 | 6.5339 | 647.26 | |
| B1-$160^0$ | 429.31 | 7.8531 | 677.39 | |

Table.11 is shown the location error of actual distance and ANN distance using the training patterns. The location error between the AFL and EFL is -1.64 (max.).

**Table.11.** Wavelet-ANN based fault location

| Type Fault | Actual Distance (km) | ANN Distance (km) | | | |
|---|---|---|---|---|---|
| | | B1 | | % error | |
| LLG (BCG) | 10 | 9.72 | 11 | 0.46 | -1.64 |
| | 20 | 19.88 | 19.58 | 0.2 | 0.7 |
| | 30 | 29.6 | 30.65 | 0.66 | -1.08 |
| | 40 | 39 | 40.80 | 1.66 | -1.33 |
| | 50 | 49 | 49.76 | 1.66 | 0.4 |

**Training data at B3 with LLG (BCG) fault**

Training patterns are formed in Table.15 with the help of data from Table.12-14.

**Table.12.** D1 Coefficients of Phase-A current at Various Distances and FIA at B3

| FIA/Km | $0^0$ | $20^0$ | $40^0$ | $60^0$ | $80^0$ | $100^0$ | $120^0$ | $140^0$ | $160^0$ |
|---|---|---|---|---|---|---|---|---|---|
| **10** | 6.8975 | 5.4701 | 7.7936 | 3.7530 | 3.9093 | 3.5245 | 3.2712 | 3.4286 | 5.3056 |
| **20** | 7.7802 | 9.2221 | 1.8856 | 3.6631 | 3.7689 | 3.5722 | 3.7710 | 3.3902 | 3.1100 |
| **30** | 3.1311 | 2.7897 | 4.0879 | 3.7910 | 4.1962 | 3.9509 | 5.0422 | 4.1357 | 4.3891 |
| **40** | 2.0868 | 8.7518 | 3.4168 | 3.6941 | 3.5451 | 3.9366 | 5.0278 | 3.7992 | 4.0208 |
| **50** | 2.4795 | 5.7869 | 3.6041 | 6.3056 | 6.1226 | 7.6875 | 7.7588 | 7.3832 | 5.9715 |

**Table.13.** D1 Coefficients of Phase-B Current at Various Distances and FIA at B3.

| FIA/Km | $0^0$ | $20^0$ | $40^0$ | $60^0$ | $80^0$ | $100^0$ | $120^0$ | $140^0$ | $160^0$ |
|---|---|---|---|---|---|---|---|---|---|
| **10** | 746.85 | 667.91 | 684.52 | 699.91 | 792.87 | 707.97 | 653.26 | 663.39 | 732.63 |
| **20** | 683.81 | 648.82 | 650.72 | 568.25 | 642.54 | 583.38 | 535.19 | 538.80 | 592.07 |
| **30** | 647.02 | 664.85 | 648.97 | 479.62 | 542.78 | 497.08 | 454.02 | 454.18 | 497.44 |
| **40** | 621.77 | 698.27 | 631.24 | 411.16 | 466.06 | 429.16 | 390.93 | 389.81 | 426.17 |
| **50** | 615.98 | 641.93 | 630.17 | 354.68 | 401.91 | 371.56 | 337.62 | 335.65 | 366.29 |

**Table.14.** D1 Coefficients of Phase-C Current at Various Distances and FIA at B3.

| FIA/Km | $0^0$ | $20^0$ | $40^0$ | $60^0$ | $80^0$ | $100^0$ | $120^0$ | $140^0$ | $160^0$ |
|---|---|---|---|---|---|---|---|---|---|
| **10** | 657.74 | 654.41 | 684.37 | 772.21 | 690.57 | 640.26 | 654.75 | 726.78 | 739.77 |
| **20** | 636.60 | 629.81 | 681.11 | 617.68 | 557.15 | 515.27 | 525.25 | 582.15 | 597.43 |
| **30** | 626.20 | 623.38 | 653.09 | 513.81 | 462.59 | 427.88 | 436.06 | 483.95 | 497.03 |
| **40** | 613.07 | 619.95 | 645.20 | 436.78 | 390.51 | 362.19 | 370.57 | 412.66 | 421.60 |
| **50** | 603.20 | 605.60 | 630.72 | 372.78 | 329.83 | 307.22 | 316.61 | 354.04 | 356.07 |

**Table.15.** Wavelet-ANN Based Fault Location

| | | | |
|---|---|---|---|
| | | ANN Distance (km) | |

| Type Fault | Actual Distance (km) | B3 | | | % error | | |
|---|---|---|---|---|---|---|---|
| LG (AG) | 1 | 0.9 | | | 1.67 | | |
| | 2 | 1.92 | | | 1.33 | | |
| | 3 | 2.98 | | | 0.33 | | |
| | 4 | 4.02 | | | -0.33 | | |
| | 5 | 5.04 | | | -0.66 | | |
| LLG (ACG) | 1 | 0.92 | 1.02 | | 1.33 | -0.33 | |
| | 2 | 2.03 | 1.98 | | -0.5 | 0.33 | |
| | 3 | 2.98 | 3.05 | | 0.33 | -0.83 | |
| | 4 | 3.92 | 3.90 | | 1.33 | 1.67 | |
| | 5 | 4.96 | 4.92 | | 0.66 | 1.33 | |
| 3-phase | 1 | 1.02 | 0.98 | 1.04 | -0.33 | 0.33 | -0.66 |
| | 2 | 1.9 | 2.08 | 2.04 | 1.66 | -1.33 | -0.66 |
| | 3 | 2.98 | 3.02 | 3.08 | 0.33 | -0.33 | -1.33 |
| | 4 | 3.98 | 3.9 | 4.10 | 0.33 | 1.67 | -1.67 |
| | 5 | 4.96 | 5.02 | 5.08 | 0.66 | -0.33 | -1.33 |
| LL (AB) | 1 | 0.92 | 1.05 | | 1.33 | -0.83 | |
| | 2 | 1.90 | 2.10 | | 1.67 | -1.66 | |
| | 3 | 2.90 | 3.04 | | 1.66 | -0.66 | |
| | 4 | 3.95 | 4.10 | | 0.83 | -1.66 | |
| | 5 | 4.90 | 5.10 | | 1.66 | -1.66 | |

Similarly, training data and training patterns are computed for bus B2, and B4 under different fault conditions. The location error of actual distance and ANN distance using training data and training patterns. The location absolute error between the AFL and EFL for LG, LLG, 3-phase and LL faults are 1.66 (max.), 1.8 (max.), 1.73 (max.) and 1.66 (max.). The D1 coefficients at random distances at B1 is also considered as testing data for the fault location error given in Table.16.

Comparison of proposed method with existing method of fault location is given in Table.17.

**Table.11.** Testing Data

| Type Fault | Actual Distance (km) | ANN Distance (km) | | | % error | | |
|---|---|---|---|---|---|---|---|
| | | B1 | | | | | |
| LG (AG) | 12 | 11.5 | | | 0.83 | | |
| | 23 | 22.3 | | | 1.16 | | |
| | 34 | 33.1 | | | 1.5 | | |
| | 45 | 44.2 | | | 1.33 | | |
| | 48 | 48.5 | | | -0.83 | | |
| LLG (ACG) | 8 | 7.8 | 8.5 | | 0.33 | -0.83 | |
| | 18 | 18.5 | 18.6 | | -0.83 | -1 | |
| | 32 | 31.8 | 32.2 | | 0.33 | --0.33 | |
| | 43 | 42.5 | 43.2 | | 0.83 | -0.33 | |
| | 54 | 53.8 | 54.6 | | 0.33 | -1 | |
| 3-phase | 9 | 8.8 | 9.2 | 9.8 | 0.33 | -0.33 | -1.33 |
| | 23 | 22.6 | 23.4 | 22.8 | 0.66 | -1 | 0.33 |
| | 32 | 31.2 | 31.6 | 31.8 | 1.33 | 0.66 | 0.33 |
| | 43 | 42 | 42.3 | 42.5 | 1.66 | 1.16 | 0.83 |
| | 54 | 53 | 53.2 | 53.4 | 1.66 | 1.33 | 1 |
| LL (BC) | 11 | 9.9 | 10.5 | | 1.83 | -0.83 | |
| | 21 | 19.8 | 20.3 | | 2 | 1.16 | |
| | 29 | 29.1 | 30.1 | | -0.16 | -0.18 | |

| | | | | | |
|---|---|---|---|---|---|
| | 45 | 44.2 | 43.8 | 1.33 | 2 |
| | 53 | 52.4 | 52.09 | 1 | 0.151 |

**Table.17.** Comparison of Proposed Method with Existing Method of Fault Location.

| S.no | Parameter | Existing method [15] | Proposed method | Observations |
|---|---|---|---|---|
| 1 | Wavelet used | Db5 level-5 | Bior1.5 level-1 | Level-1 is used |
| 2 | % error | -1.4 (50km distance)<br>2.4666 (100km distance) | -0.7333 (50km distance)<br>0.4666 (100km distance) | Better accuracy |

## 7. Conclusion

From the above analysis we can summarize the conclusions as follows

Fault location analysis of 4-bus renewable energy sources connected transmission system at distances 10km, 20km, 30km, 40km, 50km for conventional and 1km, 2km, 3km, 4km, 5km for Non-conventional sources at various faults and FIAs for various faults has been carried out and compared with existing methods. In this method the current signals are measured at both ends after the fault occurrence and the signals are decomposed by Bior1.5 mother wavelet with wavelet milt-resolution analysis and these decomposed signals further converted into D1 coefficients. These D1 coefficients are in the form of numerical values. These values (higher or lower) depend on magnitude of the fault current signals. After the D1 coefficients are obtained, ANN will be trained with these values. ANN is an ultimate tool for the location of fault using D1 coefficients. Testing data at various random distances like 12km, 23km, 34km, 45km, 48km etc. of 60km line and 1.2km, 2.1km, 3.5km, 4.6km 5.3km etc. with different faults is also developed and tested with ANN. It is found that the fault distance obtained from ANN is very closer to actual distance and the absolute error is maximum of 2% irrespective of fault impedance, fault generator capacities, fault inception angle. So that, the proposed method has shown best results for the detection of fault location of renewable energy sources integrated power transmission system.

## References

[1]. Sachit A. Gopalann, Victor Sreeram, Herbert H.C. Iu, “A review of coordination strategies and protection schemes for microgrids”, Renewable and Sustainable Energy Reviews 32(2014)222–228.

[2]. Mahmood Parsia , Peter Crossleya, Pier Luigi Dragottib , David Cole “Wavelet based fault location on power transmission lines -using real-world travelling wave data” Electric Power Systems Research, Volume 186, September 2020, 106261.

[3]. Dr. H. V. Gururaja Rao, Dr. Nagesh Prabhu, Dr. R. C. Mala “Wavelet Transform Based fault location estimator for statcom compensated lines”. Volume 11, Issue 4, June 2020, pp. 309-317.

[4]. Majid Jamila, Abul Kalama, A.Q. Ansaria, M. Rizwanba “Generalized neural network and wavelet transform based approach for fault location estimation of a transmission line” Applied Soft Computing, 19 (2014) 322–332.

[5]. A. Salehi Dobakhshari and A. M. Ranjbar “A Novel Method for Fault Location of Transmission Lines by Wide-Area Voltage Measurements Considering Measurement Errors” IEEE Transactions On Smart Grid, Vol. 6, No. 2, March 2015.

[6]. Nabamita Roy and Kesab Bhattacharya “Detection, Classification, and Estimation of Fault Location on an Overhead Transmission Line Using S-transform and Neural Network”, Electric Power Components and Systems, 43(4):461–472, 2015.

[7]. Alkım Capar, Aysen Basa Arsoy “A performance oriented impedance based fault location algorithm for series compensated transmission lines” International Journal of Electrical Power and Energy Systems 71 (2015) 209–214.

[8]. Kunjin Chen, Caowei Huang, Jinliang He “Fault detection, classification and location for transmission lines and distribution systems: a review on the methods” High Voltage., 2016, Vol. 1, Issue. 1, pp. 25–33.

[9]. J. Ren, Member, S. S. Venkata, and E. Sortomme “An Accurate Synchrophasor Based Fault Location Method for Emerging Distribution Systems” IEEE Transactions On Power Delivery, Vol. 29, No. 1, February 2014.

[10]. Gaurav Kapoor “A Discrete Wavelet Transform Approach To Fault Location On A 138kv Two Terminal Transmission Line Using Current Signals Of Both Ends” ISSN: 2395-1680 (ONLINE) ICTACT journal on microelectronics, October 2018, volume: 04, ISSUE: 03.

[11]. Luis Santiago Azuara Grande,Ricardo Granizo,Santiago Arnaltes [1]Wavelet Analysis to

Detect Ground Faults in Electrical Power Systems with Full Penetration of Converter Interface Generation' Electronics ***2023**, 12(5), 1085.*

[12]. K.P. Soman, K.I.Ramachandran, N.G.Resmi "Insight into wavelets from theory to practice" PHI publications, 3rd editon, 2010.

[13] John Abubakar and Ademola Abdulkareem 'Critical Review of Fault Detection, Fault Classification and Fault Location Techniques for Transmission Network' JOURNAL OF Engineering Science and Technology Review, 15 (2) (2022) 156 – 166.

[14]. F. B. Costa, A. H. P. Sobrinho, M. Ansaldi, and M. A. D. Almeida, "The effects of the mother wavelet for transmission line fault detection and classification," in Proc. 3rd Int. Youth Conf. Energ. (IYCE), Leiria, Portugal, Jul. 2011, pp. 1–6.

[15] Abdul Gafoor Shaik, Ramana Rao V. Pulipaka 'A new wavelet based fault detection, classification and location in transmission lines' International Journal of Electrical Power and Energy Systems 64 (2015) 35–40.